# A new instability for finite Prandtl number rotating convection with free-slip boundary conditions

Y. Ponty, T. Passot, and P. L. Sulem
*CNRS URA 1362, Observatoire de la Côte d'Azur, B.P. 229, 06304 Nice Cedex 04, France*

(Received 14 May 1996; accepted 16 September 1996)

Rolls in finite Prandtl number rotating convection with free-slip top and bottom boundary conditions are shown to be unstable with respect to small angle perturbations for any value of the rotation rate. This instability is driven by the horizontal mean flow whose estimation requires a special singular perturbation analysis. © *1997 American Institute of Physics.* [S1070-6631(97)02001-1]

## I. INTRODUCTION

Rayleigh–Bénard convection in a plane layer heated from below and rotating about a vertical axis, has been the object of special attention motivated by both astrophysical and geophysical applications, and by the existence of additional instabilities occurring in this system. In the case of free-slip top and bottom boundary conditions, Küppers and Lortz[1] showed, using a perturbation analysis near threshold, that when in an infinite Prandtl number fluid, the Taylor number (which measures the rotation rate) exceeds the critical value 2285, two-dimensional rolls are unstable with respect to perturbations of the form of a similar pattern rotated by an angle close to 58°. This instability which is also present with no-slip boundaries,[2] leads in the case of extended systems to the formation of chaotically evolving patches of parallel rolls.[3–7]

Convection at moderate Prandtl number with no-slip top and bottom boundary conditions, was addressed in Refs. 8, 2 and 9, and the Küppers–Lortz instability was shown to occur at a critical Taylor number lower than in the infinite Prandtl number limit. Free-slip boundaries were considered by Swift (cited in Ref. 9) who noted that the usual perturbative calculation of the growth rate leads to a divergence in the limit of perturbations quasi-parallel to the basic rolls. The present paper is mostly concerned with a revisited analysis of this problem, leading to a uniformly valid expression of the instability growth rate. We show in particular that for any finite Prandtl number and rotation rate, straight parallel rolls are unstable when the angle associated with the perturbation is small enough.

In Section II, steady convective rolls in a rotating frame are constructed perturbatively near threshold. Section III is devoted to the computation of the instability growth rate for finite angle perturbation, an analysis which, at finite Prandtl number, breaks down in the small angle limit. In Section IV, we present a special analysis in the resulting small angle ''boundary layer,'' where the interaction of the basic rolls with quasi-parallel perturbations leads to almost space-independent contributions which become resonant in the zero angle limit. These terms are removed by prescribing a quasi-solvability condition to the marginal mode of quasi-constant horizontal velocity. A uniform expression for the instability growth rate is then derived and a new ''small-angle instability'' is obtained. The sensitivity of the instability growth rate to the Prandtl and Taylor numbers is analyzed. Qualitative features of this instability and its nonlinear development are briefly described in Section V.

## II. STEADY CONVECTIVE ROLLS IN A ROTATING FRAME

The Boussinesq equations in a horizontal fluid layer heated from below and rotating around a vertical axis $\hat{\mathbf{z}}$, are written in the non-dimensional form

$$\Delta\mathbf{u}+\hat{\mathbf{z}}\vartheta-\nabla\Gamma-\tau\hat{\mathbf{z}}\times\mathbf{u}=P_r^{-1}\left(\mathbf{u}\cdot\boldsymbol{\nabla}\mathbf{u}+\frac{\partial}{\partial t}\mathbf{u}\right), \tag{1}$$

$$\boldsymbol{\nabla}\cdot\mathbf{u}=0, \tag{2}$$

$$\Delta\vartheta+R_a\hat{\mathbf{z}}\cdot\mathbf{u}=\mathbf{u}\cdot\boldsymbol{\nabla}\vartheta+\frac{\partial}{\partial t}\vartheta, \tag{3}$$

where the vertical diffusion time is taken as time unit. We assume a Prandtl number $P_r>0.6766$, to prevent over-stability.[10] The other parameters are the Rayleigh number $R_a$ and the square root $\tau$ of the Taylor number (equal to twice the Rossby number) which, to be specific, is taken positive (anti-clockwise rotation).

Proceeding as in Ref. 1, we introduce the operators $\Lambda=\boldsymbol{\nabla}\times(\boldsymbol{\nabla}\times\cdot)$ and $\Upsilon=\boldsymbol{\nabla}\times\cdot$, and express the velocity $\mathbf{u}=(u,v,w)^t$ in terms of two scalar fields $\phi$ and $\psi$, in the form $\mathbf{u}=\Lambda(\phi\hat{\mathbf{z}})+\Upsilon(\psi\hat{\mathbf{z}})=(\partial_z\partial_x\phi+\partial_y\psi,\partial_z\partial_y\phi-\partial_x\psi,-\Delta_h\phi)^t$, where $\Delta_h=\partial_{xx}+\partial_{yy}$. Applying the operators $\hat{\mathbf{z}}\cdot\Lambda$ and $\hat{\mathbf{z}}\cdot\Upsilon$ on Eqs. (1)–(3), we obtain

$$(U+R_aG)X=Q(X,X)+\frac{\partial}{\partial t}VX, \tag{4}$$

with

$$X=\begin{bmatrix}\phi\\ \psi\\ \vartheta\end{bmatrix},\quad Q(X,X')=\begin{bmatrix}P_r^{-1}\hat{\mathbf{z}}\cdot\Lambda(\mathbf{u}\cdot\boldsymbol{\nabla}\mathbf{u}')\\ -P_r^{-1}\hat{\mathbf{z}}\cdot\Upsilon(\mathbf{u}\cdot\boldsymbol{\nabla}\mathbf{u}')\\ \mathbf{u}\cdot\boldsymbol{\nabla}\vartheta'\end{bmatrix},$$

$$G=\begin{bmatrix}0&0&0\\ 0&0&0\\ -\Delta_h&0&0\end{bmatrix},$$

$$U=\begin{bmatrix}\Delta^2\Delta_h&-\tau\partial_z\Delta_h&-\Delta_h\\ \tau\partial_z\Delta_h&\Delta\Delta_h&0\\ 0&0&\Delta\end{bmatrix},$$

$$V=\begin{bmatrix} {P_r}^{-1}\Delta\Delta_h & 0 & 0 \\ 0 & {P_r}^{-1}\Delta_h & 0 \\ 0 & 0 & 1 \end{bmatrix}.$$

For free-slip boundary conditions, $\vartheta=\phi=\partial_{zz}\phi=\partial_z\psi=0$ in the plane $z=\pm\frac{1}{2}$.

A stationary solution of Eq. (4) is computed perturbatively near the convection threshold by expanding $R_a=R_0+\epsilon R_1+\epsilon^2 R_2+\cdots$ and $X=\epsilon X_1+\epsilon^2 X_2+\epsilon^3 X_3+\cdots$ or, more explicitly, when taking into account the boundary conditions satisfied by the individual components,

$$\phi=\epsilon\phi_1\cos\pi z+\epsilon^2\phi_2\sin 2\pi z+\cdots, \tag{5}$$

$$\psi=\epsilon\psi_1\sin\pi z+\epsilon^2(\psi_0+\psi_2\cos 2\pi z)+\cdots, \tag{6}$$

$$\vartheta=\epsilon\vartheta_1\cos\pi z+\epsilon^2\vartheta_2\sin 2\pi z+\cdots\ . \tag{7}$$

Introducing the linear operator $L=U+R_0G$, we get at the successive orders of the expansion,

$$LX_1=0, \tag{8}$$

$$LX_2=-R_1GX_1+Q(X_1,X_1), \tag{9}$$

$$LX_3=-(R_1GX_2+R_2GX_1)+Q(X_1,X_2)+Q(X_2,X_1). \tag{10}$$

For a solution in the form of two-dimensional rolls with a critical wave number $|\vec{k}_1|=k$, given by the real solution of

$$2\left(\frac{k^2}{\pi^2}\right)^3+3\left(\frac{k^2}{\pi^2}\right)^2=1+\frac{\tau^2}{\pi^4}, \tag{11}$$

the critical Rayleigh number is $R_0=[(k^2+\pi^2)^3+\tau^2\pi^2]/k^2$ (Ref. 10). To simplify the writing, we denote by

$$Z(\alpha,\beta,\gamma)=(\alpha\cos\pi z,\beta\sin\pi z,\gamma\cos\pi z)^t, \tag{12}$$

vectors corresponding to fundamental modes in the vertical direction and obeying the boundary conditions prescribed on $X$. An element of the null space of $L$ is then given by

$$v(\vec{k})=Z(c_1,c_2,c_3)e^{i\vec{k}\cdot\vec{x}}, \tag{13}$$

with $c_1=1$, $c_2=-\tau\pi/k_p^2, c_3=R_0k^2/k_p^2$, and $k_p^2=k^2+\pi^2=\sqrt{R_0/3}$, and the leading order solution reads

$$X_1=Av(\vec{k}_1)+\text{c.c.}, \tag{14}$$

where the amplitude $A$ will be determined by a solvability condition arising at a higher order. For this purpose, it is convenient to introduce the inner product

$$\langle X,X'\rangle=R_0\int\phi^*\phi' d\vec{x}+R_0\int\psi^*\psi' d\vec{x}+\int\vartheta^*\vartheta' d\vec{x}, \tag{15}$$

for which the operator $L$ is self-adjoint.

Using the notation

$$Q(X_i,X_j)+Q(X_j,X_i)=(1+\delta_{ij})(Q_{i,j}^{(1)},Q_{i,j}^{(2)},Q_{i,j}^{(3)})^t, \tag{16}$$

we have in Eq. (9),

$$Q(X_1,X_1)=\begin{bmatrix} Q_{1,1}^{(1)} \\ Q_{1,1}^{(2)} \\ Q_{1,1}^{(3)} \end{bmatrix}=\begin{bmatrix} 0 \\ 2\dfrac{\tau}{P_r}\pi^2\dfrac{k^4}{k_p^2}(A^2e^{2i\vec{k}_1\cdot\vec{x}}+\text{c.c.}) \\ -2R_0\pi\dfrac{k^4}{k_p^2}\sin 2\pi z|A|^2 \end{bmatrix}. \tag{17}$$

The solvability condition for Eq. (9) (obtained by taking the inner product of this equation with $v(\vec{k}_1)$), requires $R_1=0$. Defining the operator $P=\Delta^3+\tau^2\partial_{zz}-R_0\Delta_h$, Eq. (9) reduces to

$$\Delta_h P\phi_2=\Delta Q_{1,1}^{(1)}+\tau\partial_z Q_{1,1}^{(2)}+\Delta_h Q_{1,1}^{(3)}, \tag{18}$$

where the right hand side vanishes identically. We thus get $\Delta_h\phi_2=0$, since elements of the null space of $P$, already included in $\phi_1$, are not needed in $\phi_2$.

For the two other components of $X_2$, one easily checks that $\psi_2=0$, $\psi_0=\Psi_0e^{2i\vec{k}_1\cdot\vec{x}}+\text{c.c.}$ and $\vartheta_2=\Theta_2$ with $\Psi_0=(\tau\pi^2/8P_rk_p^2)A^2$ and $\Theta_2=(R_0k^4/2\pi k_p^2)|A|^2$. This enables us to compute

$$Q(X_1,X_2)+Q(X_2,X_1)=\begin{pmatrix} 0 \\ \dfrac{4k^4\pi}{P_r}\Psi_0(A^*e^{i\vec{k}_1\cdot\vec{x}}-3Ae^{3i\vec{k}_1\cdot\vec{x}})\sin\pi z+\text{c.c.} \\ 2\pi k^2\Theta_2Ae^{i\vec{k}_1\cdot\vec{x}}\cos\pi z\cos 2\pi z+\text{c.c.} \end{pmatrix}.$$

The solvability condition of Eq. (10) then reduces to $R_2=r_2|A|^2$ or equivalently, $\epsilon^2|A|^2=(R_a-R_0)/r_2$, with $r_2=(1/2k_p^2)(R_0k^4-(\tau^2\pi^4/{P_r}^2))$, which completes the computation of the roll amplitude in terms of the distance to threshold.

## III. THE KÜPPERS–LORTZ INSTABILITY

We assume that the steady rolls of wave vector $\vec{k}_1$ computed in Section II are subject to a perturbation $\widetilde{X}$ in the form of rolls with an infinitesimal amplitude and a wave vector $\vec{k}_2$ making with $\vec{k}_1$ an angle $\theta$ that it is enough to consider in the range $]-\pi/2,\pi/2]$. We assume for the sake of simplicity that the wave numbers $|\vec{k}_1|$ and $|\vec{k}_2|$ are critical. When real, the growth rate $\sigma$ of this perturbation is given by

$$(U+R_aG)\widetilde{X}=Q(X,\widetilde{X})+Q(\widetilde{X},X)+\sigma V\widetilde{X}. \tag{19}$$

In order to compute $\sigma=\epsilon\sigma_1+\epsilon^2\sigma_2+\cdots$ perturbatively near threshold, we also expand $\widetilde{X}=\widetilde{X}_1+\epsilon\widetilde{X}_2+\epsilon^2\widetilde{X}_3+\cdots$ or, for the individual components,

$$\widetilde{\phi}=\widetilde{\phi}_1\cos\pi z+\epsilon\widetilde{\phi}_2\sin 2\pi z+\cdots, \tag{20}$$

$$\widetilde{\psi}=\widetilde{\psi}_1\sin\pi z+\epsilon(\widetilde{\psi}_0+\widetilde{\psi}_2\cos 2\pi z)+\cdots, \tag{21}$$

$$\widetilde{\vartheta}=\widetilde{\vartheta}_1\cos\pi z+\epsilon\widetilde{\vartheta}_2\sin 2\pi z+\cdots. \tag{22}$$

Equation (19) leads to

$$L\widetilde{X}_1=0, \tag{23}$$

$$L\widetilde{X}_2=Q(X_1,\widetilde{X}_1)+Q(\widetilde{X}_1,X_1)+\sigma_1V\widetilde{X}_1, \tag{24}$$

$$L\widetilde{X}_3=Q(X_2,\widetilde{X}_1)+Q(\widetilde{X}_1,X_2)+Q(X_1,\widetilde{X}_2)+Q(\widetilde{X}_2,X_1)+\sigma_1 V\widetilde{X}_2+\sigma_2 V\widetilde{X}_1-R_2G\widetilde{X}_1. \quad (25)$$

Using a notation similar to (16), we define

$$Q(X_i,\widetilde{X}_j)+Q(\widetilde{X}_j,X_i)=Q_{i,\tilde{j}}=(Q^{(1)}_{i,\tilde{j}},Q^{(2)}_{i,\tilde{j}},Q^{(3)}_{i,\tilde{j}})^t. \quad (26)$$

Writing the solution of Eq. (23) in the form $\widetilde{X}_1=Bv(\vec{k}_2)+$c.c., where $B$ is an arbitrary constant, we have in the right-hand side of Eq. (24),

$$Q_{1,\tilde{1}}=\begin{pmatrix} \frac{j_1}{P_r}\delta_h^+\delta_h^-(AB^*e^{i\vec{k}^-\cdot\vec{x}}+ABe^{i\vec{k}^+\cdot\vec{x}})\sin 2\pi z+\text{c.c.} \\ \frac{j_2}{P_r}(\delta_h^- AB^*e^{i\vec{k}^-\cdot\vec{x}}+\delta_h^+ABe^{i\vec{k}^+\cdot\vec{x}})+\text{c.c.} \\ j_3(\delta_h^+AB^*e^{i\vec{k}^-\cdot\vec{x}}+\delta_h^-ABe^{i\vec{k}^+\cdot\vec{x}})\sin 2\pi z+\text{c.c.} \end{pmatrix}, \quad (27)$$

where we have introduced the wave vectors

$$\vec{k}^\pm=\vec{k}_1\pm\vec{k}_2, \quad (28)$$

and defined the numerical constants

$$j_1=-\frac{3}{2}\pi k^2, \quad j_2=-\frac{\tau\pi^2k^2}{k_p^2}, \quad j_3=\frac{R_0k^2\pi}{2k_p^2}. \quad (29)$$

Furthermore, the coefficient $\delta_h^\pm$ given by $\Delta_h e^{i\vec{k}^\pm\cdot\vec{x}}=\delta_h^\pm e^{i\vec{k}^\pm\cdot\vec{x}}$, reads as

$$\delta_h^+=-4k^2\cos^2\frac{\theta}{2}, \quad \delta_h^-=-4k^2\sin^2\frac{\theta}{2}. \quad (30)$$

Since $\langle v(\vec{k}_2),Q(X_1,\widetilde{X}_1)+Q(\widetilde{X}_1,X_1)\rangle=0$, while $\langle v(\vec{k}_2),V\widetilde{X}_1\rangle\neq 0$, the solvability condition for Eq. (24) implies $\sigma_1=0$. Straightforward algebra then leads to

$$P\Delta_h\widetilde{\phi}_2=\Delta Q^{(1)}_{1,\tilde{1}}+\tau\partial_z Q^{(2)}_{1,\tilde{1}}+\Delta_h Q^{(3)}_{1,\tilde{1}}, \quad (31)$$

$$\Delta\Delta_h\widetilde{\psi}_2=-\tau\partial_z\Delta_h\widetilde{\phi}_2, \quad (32)$$

$$\Delta\Delta_h\widetilde{\psi}_0=Q^{(2)}_{1,\tilde{1}}, \quad (33)$$

$$\Delta\widetilde{\vartheta}_2=Q^{(3)}_{1,\tilde{1}}+R_0\Delta_h\widetilde{\phi}_2. \quad (34)$$

Solving in the form

$$\widetilde{\phi}_2=\widetilde{\Phi}_2^+ABe^{i\vec{k}^+\cdot\vec{x}}+\widetilde{\Phi}_2^-AB^*e^{i\vec{k}^-\cdot\vec{x}}+\text{c.c.}, \quad (35)$$

$$\widetilde{\psi}_2=\widetilde{\Psi}_2^+ABe^{i\vec{k}^+\cdot\vec{x}}+\widetilde{\Psi}_2^-AB^*e^{i\vec{k}^-\cdot\vec{x}}+\text{c.c.}, \quad (36)$$

$$\widetilde{\psi}_0=\widetilde{\Psi}_0^+ABe^{i\vec{k}^+\cdot\vec{x}}+\widetilde{\Psi}_0^-AB^*e^{i\vec{k}^-\cdot\vec{x}}+\text{c.c.}, \quad (37)$$

$$\widetilde{\vartheta}_2=\widetilde{\Theta}_2^+ABe^{i\vec{k}^+\cdot\vec{x}}+\widetilde{\Theta}_2^-AB^*e^{i\vec{k}^-\cdot\vec{x}}+\text{c.c.}, \quad (38)$$

we get

$$\widetilde{\Phi}_2^+=\frac{\delta_h^-}{p^+}\left(\frac{j_1}{P_r}\delta^++j_3\right), \quad \widetilde{\Phi}_2^-=\frac{\delta_h^+}{p^-}\left(\frac{j_1}{P_r}\delta^-+j_3\right),$$

$$\widetilde{\Psi}_2^+=-2\pi\tau\frac{\delta_h^-}{p^+\delta^+}\left(\frac{j_1}{P_r}\delta^++j_3\right),$$

$$\widetilde{\Psi}_2^-=-2\pi\tau\frac{\delta_h^+}{p^-\delta^-}\left(\frac{j_1}{P_r}\delta^-+j_3\right),$$

$$\widetilde{\Psi}_0^+=\frac{j_2}{P_r\delta_h^+}, \quad \widetilde{\Psi}_0^-=\frac{j_2}{P_r\delta_h^-},$$

$$\widetilde{\Theta}_2^+=R_0\frac{\delta_h^+\delta_h^-}{p^+\delta^+}\left(\frac{j_1}{P-r}\delta^++j_3\right)+j_3\frac{\delta_h^-}{\delta^+},$$

$$\widetilde{\Theta}_2^-=R_0\frac{\delta_h^+\delta_h^-}{p^-\delta^-}\left(\frac{j_1}{P_r}\delta^-+j_3\right)+j_3\frac{\delta_h^+}{\delta^-}.$$

The coefficient $\delta^\pm$ and $p^\pm$ defined by the condition $\Delta e^{i\vec{k}^\pm\cdot\vec{x}}T(2\pi z)=\delta^\pm e^{i\vec{k}^\pm\cdot\vec{x}}T(2\pi z)$ and $Pe^{i\vec{k}^\pm\cdot\vec{x}}T(2\pi z)=p^\pm e^{i\vec{k}^\pm\cdot\vec{x}}T(2\pi z)$, (where the function $T$ stands for sine or cosine), are given by

$$\delta^+=-\left[4\pi^2+4k^2\cos^2\frac{\theta}{2}\right], \quad (39)$$

$$\delta^-=-\left[4\pi^2+4k^2\sin^2\frac{\theta}{2}\right], \quad (40)$$

$$p^+=-\left[4\pi^2+4k^2\cos^2\frac{\theta}{2}\right]^3-4\pi^2\tau^2+4k^2R_0\cos^2\frac{\theta}{2}, \quad (41)$$

$$p^-=-\left[4\pi^2+4k^2\sin^2\frac{\theta}{2}\right]^3-4\pi^2\tau^2+4k^2R_0\sin^2\frac{\theta}{2}, \quad (42)$$

where the $\cos^2\theta/2$ and $\sin^2\theta/2$ contributions result from the action of the horizontal Laplacian on $e^{i\vec{k}^+\cdot\vec{x}}$ and $e^{i\vec{k}^-\cdot\vec{x}}$ respectively.

An important observation is that the contribution $\widetilde{\Psi}_0^- AB^*e^{i\vec{k}^-\cdot\vec{x}}$ to $\widetilde{\psi}_2$ (which disappears at infinite Prandtl number) diverges in the limit $\theta\to 0$, where it can be viewed as associated to a ''mean flow'' generated by the rotation. This term is specific to free-slip boundary conditions and has no equivalent when rigid boundaries are considered. The divergence originates from the fact that in Eqs. (31)–(34), the dynamics of the mean flow is slaved to that of the leading convective mode. This ''adiabatic approximation'' is valid at finite $\theta$ but breaks down in an ''angular boundary layer'' near $\theta=0$, where time derivatives become relevant. Postponing to Section IV the analysis of this layer, we derive here the solvability condition of Eq. (25) for finite $\theta$, by writing

$$\langle v(\vec{k}_2),G\widetilde{X}_1\rangle=\tfrac{1}{2}c_1c_3k^2B^*, \quad (43)$$

$$\langle v(\vec{k}_2),V\widetilde{X}_1\rangle=\tfrac{1}{2}(R_0{P_r}^{-1}c_1^2k^2{k_p}^2-R_0{P_r}^{-1}c_2^2k^2+c_3^2)B^*, \quad (44)$$

$$\langle v(\vec{k}_2),(Q(X_2,\widetilde{X}_1)+Q(\widetilde{X}_1,X_2)\rangle=\tfrac{1}{4}c_1^2c_3^2k^4|A|^2B^*. \quad (45)$$

Furthermore

$$Q(X_1,\widetilde{X}_2)+Q(\widetilde{X}_2,X_1)=Z(q^{(1)}_{1,\tilde{2}},q^{(2)}_{1,\tilde{2}},q^{(3)}_{1,\tilde{2}})|A|^2B^*\times e^{-i\vec{k}_2\cdot\vec{x}}+\text{c.c.}+F_3, \quad (46)$$

where $F_3$ refers to non-resonant terms proportional to $\sin 3\pi z$ or $\cos 3\pi z$. We also have

$$q_{1,\tilde{2}}^{(1)}=\frac{k^4}{2P_r}\sin\theta[(-\tilde{\Psi}_2^{+}+2\tilde{\Psi}_0^{-})(c_1\pi^2-c_1k^2-2c_1\pi^2\cos\theta-2c_2\pi\sin\theta)+(\tilde{\Psi}_2^{-}-2\tilde{\Psi}_0^{+})(c_1\pi^2-c_1k^2+2c_1\pi^2\cos\theta+2c_2\pi\sin\theta)+2\tilde{\Phi}_2^{-}k_p^2(c_2(1-\cos\theta)+\pi c_1\sin\theta)-2\tilde{\Phi}_2^{+}k_p^2(c_2(1+\cos\theta)-\pi c_1\sin\theta)], \tag{47}$$

$$q_{1,\tilde{2}}^{(2)}=-\frac{k^4}{2P_r}[2\tilde{\Psi}_0^{-}(c_1\pi(-1+2\cos\theta-\cos 2\theta)+c_2(\sin\theta-\sin 2\theta))+2\tilde{\Psi}_0^{+}(c_1\pi(-1-2\cos\theta-\cos 2\theta)-c_2(\sin\theta+\sin 2\theta))+\tilde{\Psi}_2^{+}\sin\theta(-2c_1\pi\sin\theta+c_2(1+2\cos\theta))+\tilde{\Psi}_2^{-}\sin\theta(-2c_1\pi\sin\theta-c_2(1-2\cos\theta))+\tilde{\Phi}_2^{+}(c_2\pi(1-\cos 2\theta)-\pi^2c_1(2\sin\theta-\sin 2\theta))+\tilde{\Phi}_2^{-}(c_2\pi(1-\cos 2\theta)+\pi^2c_1(2\sin\theta+\sin 2\theta))], \tag{48}$$

$$q_{1,\tilde{2}}^{(3)}=\frac{k^2}{2}[\tilde{\Theta}_2^{-}(c_1\pi(1+\cos\theta)+c_2\sin\theta)+\tilde{\Theta}_2^{+}(c_1\pi(1-\cos\theta)-c_2\sin\theta)]+\frac{k^2}{2}c_3[\tilde{\Psi}_2^{+}+2\tilde{\Psi}_0^{+}-\tilde{\Psi}_2^{-}-2\tilde{\Psi}_0^{-}]\sin\theta. \tag{49}$$

It follows that

$$\langle v(\vec{k}_2),Q(X_1,\tilde{X}_2)+Q(\tilde{X}_2,X_1)\rangle=\tfrac{1}{2}(R_0c_1q_{1,\tilde{2}}^{(1)}+R_0c_2q_{1,\tilde{2}}^{(2)}+c_3q_{1,\tilde{2}}^{(3)})|A|^2B^*, \tag{50}$$

and finally

$$\sigma=\epsilon^2\sigma_2=\epsilon^2\frac{r_2c_1c_3k^2-\left(\frac{1}{2}c_1^2c_3^2k^4+R_0c_1q_{1,\tilde{2}}^{(1)}+R_0c_2q_{1,\tilde{2}}^{(2)}+c_3q_{1,\tilde{2}}^{(3)}\right)}{R_0P_r{}^{-1}c_1^2k^2k_p{}^2-R_0P_r{}^{-1}c_2^2k^2+c_3^2}|A|^2, \tag{51}$$

where $\epsilon^2|A|^2$ can be expressed as

$$\frac{2k_p^2}{R_0k^4-\frac{\tau^2\pi^4}{P_r^2}}(R_a-R_0).$$

Since in the limit $\theta\to 0$, $\tilde{\Psi}_0^{-}$ diverges like $\sin^{-2}\theta/2$, the quantity $q_{1,\tilde{2}}^{(l)}$ with $l=1,2,3$, scales like $\sin\theta/2\,\tilde{\Psi}_0^{-}\sim\sin^{-1}\theta/2$, and the growth rate behaves like

$$\sigma\sim\frac{\tau\pi^2k^2|A|^2}{2k_p^2P_r}\frac{\epsilon^2}{\sin\frac{\theta}{2}}, \tag{52}$$

indicating a breakdown of the above asymptotics at finite Prandtl numbers, in the case of small angle perturbations.

Pushing the $\theta$-expansion at the next order (as needed in Section IV), we write

$$\sigma\sim\left[-\eta+\frac{\tau\pi^2k^2}{2k_p^2P_r}\left(2\xi+\frac{1}{\sin\frac{\theta}{2}}\right)\right]\epsilon^2|A|^2, \tag{53}$$

with

$$\eta=\frac{r_2}{R_0}\frac{k_p^2}{\left(1+\frac{1}{P_r}\left(1-\frac{2\tau^2\pi^2}{R_0k^2}\right)\right)} \tag{54}$$

and

$$\xi=-\frac{\tau\pi^2}{P_rk_p^2k^2\left(1+\frac{1}{P_r}\left(1-\frac{2\tau^2\pi^2}{R_0k^2}\right)\right)}, \tag{55}$$

the latter coefficient collecting contributions originating from $\tilde{\Psi}_0^{-}$.

The divergence shown in Eq. (52) was noted in Ref. 9. It indicates that the above analysis should be viewed as an outer expansion, and that a different scaling is required for small $\theta$. In the following, the growth rate given by Eq. (51) will thus be denoted $\sigma_{outer}$.

## IV. THE SMALL-ANGLE INSTABILITY

The small angle divergence of the stream function $\psi_0\sim\epsilon\sin^{-2}\theta/2$ and of the growth rate $\sigma_{outer}\sim\epsilon^2\sin^{-1}\theta/2$, indicates that new scalings in $\epsilon$ are expected in an angular boundary layer near $\theta=0$. Denoting by $\epsilon^\alpha$ the thickness of this layer, by $\epsilon^\beta$ the amplitude of $\Psi_0$ and by $\epsilon^\gamma$ the magnitude of the growth rate in this layer, the matching of the ''outer'' and ''inner'' regions requires $\beta=1-2\alpha$ and $\gamma=2-\alpha$. Since, in the inner region, the time derivative in the mean flow equation (whose presence will remove the divergence) becomes comparable to the viscous term when $\gamma=2\alpha$, we get $\alpha=\frac{2}{3}$, $\beta=-\frac{1}{3}$ and $\gamma=\frac{4}{3}$.

Furthermore, when expanding Eq. (4) inside the boundary layer, the parameter $\epsilon$ appears not only through the horizontal Fourier modes of $X_1$ whose amplitudes scale like entire powers of $\epsilon$, but also through the angular dependence of the operators involved in this equation. We are thus led to expand

$$\sigma=\epsilon\sigma_1+\epsilon^{4/3}\sigma_{4/3}+\epsilon^{5/3}\sigma_{5/3}+\epsilon^2\sigma_2+\epsilon^{7/3}\sigma_{7/3}+\epsilon^{8/3}\sigma_{8/3}+\cdots \tag{56}$$

and

$$\widetilde{X}=\epsilon^{-1/3}\widetilde{Y}_{-1/3}+\widetilde{Y}_0+\widetilde{X}_1+\epsilon^{1/3}\widetilde{Y}_{1/3}+\epsilon^{2/3}\widetilde{Y}_{2/3}+\epsilon\widetilde{X}_2$$
$$+\epsilon^{4/3}\widetilde{X}_{4/3}+\epsilon^{5/3}\widetilde{X}_{5/3}+\epsilon^2\widetilde{X}_3+\epsilon^{7/3}\widetilde{X}_{7/3}$$
$$+\epsilon^{8/3}\widetilde{X}_{8/3}+\epsilon^3\widetilde{X}_4+\cdots, \tag{57}$$

where terms of the form $\widetilde{Y}_\mu=\widetilde{\Psi}_\mu B^*Ae^{i\vec{k}^-\cdot\vec{x}}(0,1,0)^t+\text{c.c.}$, are introduced to cancel almost resonant contributions resulting from the interaction of the basic rolls with quasi-parallel perturbations. As seen later, in the boundary layer, $\sigma$ can be complex.

Substituting (57) and (56) in Eq. (19) and concentrating on perturbations such that the angle $\theta$ between the wave vectors $\vec{k}_1$ and $\vec{k}_2$ is of order $\epsilon^{2/3}$, we obtain the following hierarchy.

At order $\epsilon^0$,

$$L\widetilde{X}_1=0, \tag{58}$$

leading to

$$\widetilde{X}_1=v(\vec{k}_2)B+\text{c.c.} \tag{59}$$

At order $\epsilon$,

$$L\widetilde{X}_2=\begin{pmatrix} 0 \\ -\dfrac{4j_2k^2}{P_r}ABe^{i\vec{k}^+\cdot\vec{x}} \\ -4j_3k^2AB^*e^{i\vec{k}^-\cdot\vec{x}}\sin 2\pi z \end{pmatrix}$$
$$+\sigma_1BVv(\vec{k}_2)+\text{c.c.} \tag{60}$$

The solvability condition reads

$$\epsilon\sigma_1=0, \tag{61}$$

and the solution is given by

$$\widetilde{X}_2=\begin{pmatrix} 0 \\ \widetilde{\Psi}_0^+ABe^{i\vec{k}^+\cdot\vec{x}} \\ \widetilde{\Theta}_2^-AB^*e^{i\vec{k}^-\cdot\vec{x}}\sin 2\pi z \end{pmatrix}+\text{c.c.} \tag{62}$$

with $\widetilde{\Psi}_0^+=-j_2/4k^2P_r$ and $\widetilde{\Theta}_2^-=j_3(k^2/\pi^2)$.

At order $\epsilon^{4/3}$,

$$\epsilon^{4/3}L\widetilde{X}_{4/3}=\epsilon^{2/3}\sin\theta\widetilde{\Psi}^*_{-1/3}|A|^2Be^{i\vec{k_2}\cdot\vec{x}}$$
$$\times Z\left(-\frac{k^4k_p^2}{P_r},\frac{k^4c_2}{P_r},-k^2c_3\right)$$
$$+\epsilon^{4/3}\sigma_{4/3}VBv(\vec{k}_2)+\text{c.c.}+\mathcal{NR}, \tag{63}$$

where $\mathcal{NR}$ collects non-resonant terms. The solvability condition is

$$\epsilon^{4/3}\sigma_{4/3}=\epsilon k^2\sin\theta|A|^2\epsilon^{-1/3}\widetilde{\Psi}^*_{-1/3}. \tag{64}$$

At order $\epsilon^{5/3}$,

$$\epsilon^{5/3}L\widetilde{X}_{5/3}=\epsilon\sin\theta\widetilde{\Psi}_0^*|A|^2Be^{i\vec{k_2}\cdot\vec{x}}$$
$$\times Z\left(-\frac{k^4k_p^2}{P_r},\frac{k^4c_2}{P_r},-k^2c_3\right)$$
$$+\epsilon^{5/3}\sigma_{5/3}VBv(\vec{k}_2)+\text{c.c.}+\mathcal{NR}. \tag{65}$$

The solvability of this equation requires

$$\epsilon^{5/3}\sigma_{5/3}=\epsilon k^2\sin\theta|A|^2\widetilde{\Psi}_0^*. \tag{66}$$

At order $\epsilon^2$,

$$\epsilon^2L\widetilde{X}_3=\epsilon^2Q_{\bar{1},2}+\epsilon^2Z(\overline{q_{1,\bar{2}}^{(1)}},\overline{q_{1,\bar{2}}^{(2)}},\overline{q_{1,\bar{2}}^{(3)}})|A|^2Be^{i\vec{k_2}\cdot\vec{x}}$$
$$+\epsilon^{2/3}\sin\theta\widetilde{\Psi}^*_{-1/3}e^{i\vec{k_2}\cdot\vec{x}}|A|^2BZ$$
$$\times\left(-2\frac{k^4}{P_r}c_2\pi\sin\theta,\frac{k^4}{P_r}c_1\pi\left(\sin\frac{\theta}{2}-\sin\frac{3\theta}{2}\right),0\right)$$
$$+\epsilon^{4/3}\sin\theta\widetilde{\Psi}^*_{1/3}|A|^2Be^{i\vec{k_2}\cdot\vec{x}}Z\left(-\frac{k^4k_p^2}{P_r},\frac{k^4c_2}{P_r},-k^2c_3\right)$$
$$-\epsilon^2R_2G\widetilde{X}_1+\epsilon^2\sigma_2VBv(\vec{k}_2)+\text{c.c.}+\mathcal{NR}, \tag{67}$$

where

$$(\overline{q_{1,\bar{2}}^{(1)}},\overline{q_{1,\bar{2}}^{(2)}},\overline{q_{1,\bar{2}}^{(3)}})=\left(0,4\frac{k^4}{P_r}c_1\pi\widetilde{\Psi}_0^+,k^2c_1\pi\widetilde{\Theta}_2^-\right) \tag{68}$$

denotes the limit as $\theta\to 0$ of the vector $(q_{1,\bar{2}}^{(1)},q_{1,\bar{2}}^{(2)},q_{1,\bar{2}}^{(3)})$ from which the contributions coming from $\Psi_0^-$ have been removed. The solvability condition reads

$$\epsilon^2\sigma_2=-\eta|A|^2\epsilon^2+2\epsilon^{2/3}\xi k^2\sin\theta\sin\frac{\theta}{2}|A|^2\widetilde{\Psi}^{-*}_{-1/3}$$
$$+\epsilon^{4/3}k^2\sin\theta|A|^2\widetilde{\Psi}^{-*}_{1/3}, \tag{69}$$

where

$$\eta=-\frac{r_2c_1c_3k^2-\left(\dfrac{1}{2}c_1^2c_3^2k^4+R_0c_1\overline{q_{1,\bar{2}}^{(1)}}+R_0c_2\overline{q_{1,\bar{2}}^{(2)}}+c_3\overline{q_{1,\bar{2}}^{(3)}}\right)}{R_0P_r{}^{-1}c_1^2k^2k_p{}^2-R_0P_r{}^{-1}c_2^2k^2+c_3^2} \tag{70}$$

identifies with the expression given in Eq. (54). The coefficient $\xi$ is given by Eq. (55).

Combining the solvability conditions (61), (64), (66), and (69), we are led to express the growth rate

$$\sigma_{inner}=\epsilon^{4/3}\sigma_{4/3}+\epsilon^{5/3}\sigma_{5/3}+\epsilon^2\sigma_2, \tag{71}$$

in terms of the ‘‘mean flow’’

$$\Psi=\epsilon^{-1/3}\widetilde{\Psi}^*_{-1/3}+\widetilde{\Psi}_0^*+\epsilon^{1/3}\widetilde{\Psi}^*_{1/3}, \tag{72}$$

in the form

$$\sigma_{inner}=\epsilon k^2\sin\theta|A|^2\left(1+2\xi\sin\frac{\theta}{2}\right)\Psi-\epsilon^2\eta|A|^2, \tag{73}$$

where subdominant corrections have been neglected.

In order to estimate the mean flow $\Psi$, we push the $\epsilon$-expansion of Eq. (4) at higher orders, where the beating of the perturbation with the basic solution produces contributions of the form $e^{i(\vec{k}_1-\vec{k}_2)\cdot\vec{x}}$ which become space-independent and thus resonant in the small $\theta$ limit. Consequently, uniform boundedness of the solutions requires, in addition to the usual solvability conditions, the prescription of ‘‘quasi-solvability conditions’’ aimed to eliminate terms which are strictly resonant only for $\theta=0$. This approach is similar to that used by Ablowitz and Benney[11] when dealing with the small-amplitude divergence of the Whitham modulation analysis for non-linear dispersive waves (see also Ref. 12). These authors modify the (algebraic) dispersion relation by means of additional corrective terms determined by a constraint which becomes an actual solvability condition in the small amplitude limit, thus transforming the algebraic dispersion relation arising in Whitham's theory, into a partial differential equation for the wave amplitude. In the context of rotating convection, we include contributions $\widetilde{Y}_n$ proportional to $e^{i(\vec{k}_1-\vec{k}_2)\cdot\vec{x}}$ in the perturbation expansion, which are determined by cancelling them with the terms displaying the same functional dependence and originating from the beating of the basic rolls with quasi-parallel perturbations. Like in the small-amplitude limit of non-linear waves, this condition becomes an actual solvability in the limit $\theta\rightarrow 0$. In both instances, the singularity is prevented by removing slaving conditions: that of the amplitude with respect to the phase in the case of waves, or that of the mean flow with respect to the convective modes in the present problem [compare Eqs. (32) and (80) below].

At order $\epsilon^{7/3}$,

$$\epsilon^{7/3}L\widetilde{X}_{7/3}+\begin{pmatrix}\epsilon\delta_h^-\widetilde{\Theta}_2^- AB^*e^{i\vec{k}^-\cdot\vec{x}}\sin 2\pi z\\ \epsilon^{-1/3}\delta_h^{-2}\widetilde{\Psi}_{-1/3}AB^*e^{i\vec{k}^-\cdot\vec{x}}+\text{c.c.}\\ 0\end{pmatrix}$$

$$=\epsilon^{7/3}[Q_{1,\widetilde{4/3}}]+\epsilon\begin{pmatrix}\frac{j_1}{P_r}\delta_h^+\delta_h^-(AB^*e^{i\vec{k}^-\cdot\vec{x}}+ABe^{i\vec{k}^+\cdot\vec{x}})\sin 2\pi z+\text{c.c.}\\ \frac{j_2}{P_r}\delta_h^- AB^*e^{i\vec{k}^-\cdot\vec{x}}+\text{c.c.}\\ j_3\delta_h^- ABe^{i\vec{k}^+\cdot\vec{x}}\sin 2\pi z+\text{c.c.}\end{pmatrix}+\begin{pmatrix}0\\ \epsilon^{4/3}\sigma_{4/3}^*P_r^{-1}\delta_h^-\epsilon^{-1/3}\widetilde{\Psi}_{-1/3}AB^*e^{i\vec{k}^-\cdot\vec{x}}+\text{c.c.}\\ 0\end{pmatrix}$$

$$+\epsilon\sin\theta\widetilde{\Psi}_0^*e^{i\vec{k}_2\cdot\vec{x}}|A|^2BZ\left(-2\frac{k^4}{P_r}c_2\pi\sin\theta,\frac{k^4}{P_r}c_1\pi\left(\sin\frac{\theta}{2}-\sin\frac{3\theta}{2}\right),0\right)+\epsilon^{5/3}\sin\theta\widetilde{\Psi}_{2/3}^*Ae^{i\vec{k}_2\cdot\vec{x}}Z\left(-\frac{k^4k_p^2}{P_r},\frac{k^4c_2}{P_r},-k^2c_3\right)$$

$$+\epsilon^{7/3}\sigma_{4/3}V\widetilde{X}_2+\epsilon^{7/3}\sigma_{7/3}V\widetilde{X}_1, \tag{74}$$

where $[Q_{1,\widetilde{4/3}}]$ denotes the leading order of $Q(X_1,\widetilde{X}_{4/3})+Q(\widetilde{X}_{4/3},X_1)$. Although $\widetilde{X}_{4/3}$ contains terms proportional to $e^{\pm i\vec{k}_2\cdot\vec{x}}$, the resulting contributions of the form $e^{i\vec{k}^-\cdot\vec{x}}$ in $Q_{1,\widetilde{4/3}}$ are preceded by a factor proportional to $\sin^2\theta/2$ and thus not included in $[Q_{1,\widetilde{4/3}}]$. The quasi-solvability condition then reads

$$-\epsilon\sigma_{4/3}P_r^{-1}\delta_h^-\widetilde{\Psi}_{-1/3}^*+\epsilon^{-1/3}\delta_h^{-2}\widetilde{\Psi}_{-1/3}^*-\epsilon\delta_h^- j_2P_r^{-1}=0. \tag{75}$$

At order $\epsilon^{8/3}$,

$$\epsilon^{8/3}L\widetilde{X}_{8/3}+\begin{pmatrix}0\\ -P_r^{-1}\delta_h^-\epsilon^{4/3}\sigma_{4/3}\widetilde{\Psi}_0^*+\delta_h^{-2}\widetilde{\Psi}_0^*-P_r^{-1}\epsilon^{4/3}\sigma_{5/3}\widetilde{\Psi}_{-1/3}^*\\ 0\end{pmatrix}$$

$$=[Q_{\widetilde{5/3},1}]+\begin{pmatrix}0\\ \epsilon^2\frac{8}{P_r}k^4\Psi_0(B\epsilon^{-1/3}\widetilde{\Psi}_{-1/3}^*e^{i\vec{k}^+\cdot\vec{x}}+\text{c.c.})\sin\theta\cos^2\frac{\theta}{2}\\ 0\end{pmatrix}+\epsilon^{4/3}\sin\theta\widetilde{\Psi}_{1/3}^*e^{i\vec{k}_2\cdot\vec{x}}|A|^2BZ$$

$$\times\left(-2\frac{k^4}{P_r}c_2\pi\sin\theta,\frac{k^4}{P_r}c_1\pi\left(\sin\frac{\theta}{2}-\sin\frac{3\theta}{2}\right),0\right). \tag{76}$$

The quasi-solvability condition is

$$-P_r^{-1}\epsilon^{-4/3}\sigma_{4/3}\delta_h^-\widetilde{\Psi}_0^*+\delta_h^{-2}\widetilde{\Psi}_0^*-P_r^{-1}\epsilon^{5/3}\sigma_{5/3}\delta_h^-(\epsilon^{-1/3}\widetilde{\Psi}_{-1/3}^*)=0 \tag{77}$$

where, as previously, $[Q_{\widetilde{5/3},1}]$ does not contribute.

At order $\epsilon^3$,

$$\epsilon^3L\widetilde{X}_4=\epsilon^3[Q_{1,\widetilde{3}}+Q_{3,\widetilde{1}}+Q_{2,\widetilde{2}}]-\epsilon^3R_3G\widetilde{X}_1-\epsilon^3R_2G\widetilde{X}_2+\epsilon^3(\sigma_2V\widetilde{X}_2+\sigma_3V\widetilde{X}_1)-(0,\epsilon^{1/3}\delta_h^{-2}\widetilde{\Psi}_{1/3}^*AB^*e^{-i\vec{k}^-\cdot\vec{x}}+\text{c.c.},0)^t$$

$$+(0,P_r^{-1}\delta_h^-\epsilon^{5/3}(\sigma_2\widetilde{\Psi}_{-1/3}^*+\sigma_{4/3}\widetilde{\Psi}_{1/3}^*+\sigma_{5/3}\widetilde{\Psi}_0^*)AB^*e^{-i\vec{k}^-\cdot\vec{x}}+\text{c.c.},0)^t, \tag{78}$$

with the quasi-solvability condition

$$\delta_h^{-2}(\epsilon^{1/3}\tilde{\Psi}_{1/3}^{-*})-P_r^{-1}\epsilon^2\sigma_2\delta_h^-(\epsilon^{-1/3}\tilde{\Psi}_{-1/3}^*)$$
$$-P_r^{-1}\epsilon^{4/3}\sigma_{4/3}\delta_h^-(\epsilon^{1/3}\tilde{\Psi}_{1/3}^*)-P_r^{-1}\epsilon^{5/3}\sigma_{5/3}\delta_h^-\tilde{\Psi}_0^*=0. \tag{79}$$

Combining Eqs. (75), (77) and (79), we get, up to subdominant contributions,

$$-P_r^{-1}\sigma_{inner}\Psi+\delta_h^-\Psi=\epsilon P_r^{-1}j_2 \tag{80}$$

which together with Eq. (73), constitute a closed system. Solving the resulting quadratic equation for the growth rate, we obtain two solutions

$$\sigma_{inner}^{\pm}=\frac{1}{2}\left(-\epsilon^2\eta|A|^2-4k^2P_r\sin^2\frac{\theta}{2}\right)$$
$$\pm\frac{1}{2}\left[\left(\epsilon^2\eta|A|^2-4k^2P_r\sin^2\frac{\theta}{2}\right)^2-4\epsilon^2k^2\sin\theta|A|^2j_2\left(1+2\sin\frac{\theta}{2}\xi\right)\right]^{1/2}, \tag{81}$$

where $\eta$, $\xi$ and $j_2$ are defined by Eqs. (54), (55) and (29). This expression covers several regimes.

(i) For $\theta\sim\epsilon^{2/3}$,

$$\sigma_{inner}^{\pm}\sim\frac{1}{2}\left(-4k^2P_r\sin^2\frac{\theta}{2}\right)\pm\frac{1}{2}\left[\left(4k^2P_r\sin^2\frac{\theta}{2}\right)^2-4\epsilon^2k^2\sin\theta|A|^2j_2\right]^{1/2}. \tag{82}$$

In this range, $\sigma_{inner}^+>0$ for $\theta>0$ ($\theta<0$) if $\tau>0$ (respectively, $\tau<0$) for any finite value of the Prandtl number (still assuming $P_r>0.6766$) and of the Taylor number.

(ii) When $\theta\gg\epsilon^{2/3}$,

$$\sigma_{inner}^+\sim\sigma_{match}=\left[-\eta+\frac{\tau\pi^2k^2}{2k_p^2P_r}\left(2\xi+\frac{1}{\sin\frac{\theta}{2}}\right)\right]\epsilon^2|A|^2, \tag{83}$$

and matches the limit of $\sigma_{outer}$ as $\theta\to0$. Similarly,

$$\sigma_{inner}^-\sim-4k^2P_r\sin^2\frac{\theta}{2} \tag{84}$$

is negative and becomes of order unity outside the boundary layer.

(iii) For $\theta\sim\epsilon^2$,

$$\sigma_{inner}^{\pm}\sim\tfrac{1}{2}(-\epsilon^2\eta|A|^2)\pm\tfrac{1}{2}[(\epsilon^2\eta|A|^2)^2-4\epsilon^2k^2\sin\theta|A|^2j_2]^{1/2}, \tag{85}$$

and for $\theta=0$, $\sigma_{inner}^+$ vanishes, while $\sigma_{inner}^-(0)=-\epsilon^2\eta|A|^2$.

We thus obtain a uniform representation for $\theta\in]-\pi/2,\pi/2]$, of the instability growth rate near the convection threshold, of the form

$$\sigma^+=\sigma_{inner}^++\sigma_{outer}-\sigma_{match}, \tag{86}$$

where the various terms arising in the right-hand-side of Eq. (86) are given by Eqs. (51), (81) and (83). The influence of various parameters like the Prandtl number and the rotation rate on the strength of the instability, is illustrated in the following figures.

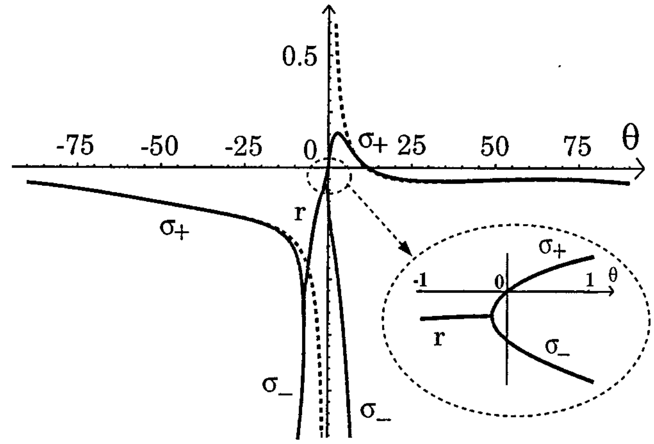


FIG. 1. Instability growth rates $\sigma^+$ and $\sigma^-$ or their real part $r$ when complex conjugate (full line), together with the diverging ''outer solution'' (dashed line), versus the perturbation angle $\theta$ (in degrees), for $P=10$, $\tau=10$ and $\epsilon=0.1$.

Figure 1 shows the variation of the eigenvalues $\sigma^{\pm}$ with the angle $\theta$ of the perturbation for $P_r=2$, $\epsilon=0.1$ and $\tau=10$. For anti-clockwise rotation and finite Prandtl number, the growth rate $\sigma^+$ is positive for small enough positive angles $\theta$. There is also a range of negative angles, where there are two complex conjugate eigenvalues, with negative real parts. The dashed line represents the outer solution $\sigma_{outer}$ which diverges in the limit $\theta\to0$. The other eigenvalue $\sigma^-$ which, as $\epsilon\to0$, becomes marginal in a neighborhood of $\theta=0$, is of order unity outside the angular boundary layer. It thus cannot be computed perturbatively for $\theta$ of order unity but, being always negative or complex with a negative real part, it cannot lead to an instability.

Figure 2 displays the growth rate $\sigma^+$ for $\tau=38$, $\epsilon=0.1$ and various values of the Prandtl number for positive angles. We observe that both the range of unstable angles and the

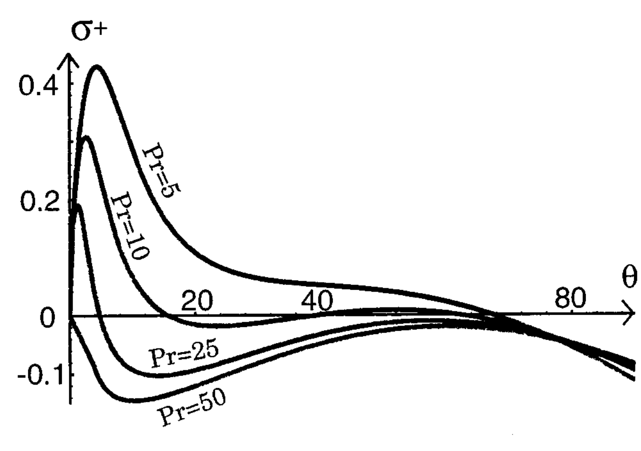


FIG. 2. Growth rate $\sigma^+$, versus the perturbation angle $\theta>0$, for $\tau=38$, $\epsilon=0.1$ and different values $P_r=5,10,25,50$ of the Prandtl number.

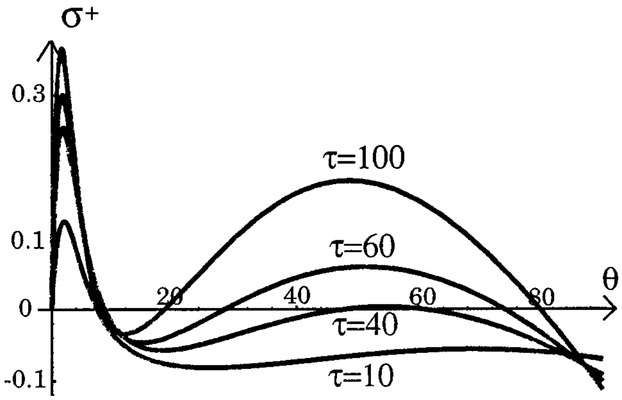


FIG. 3. Growth rate $\sigma^+$, versus the perturbation angle $\theta > 0$, for $P = 15$, $\epsilon = 0.1$ and different values $\tau = 10$, 40, 60, 100 of the rotation rate $\tau$.

maximal growth rate decrease when the Prandtl number is increased. At $P_r = 10$, the small angle instability and the Küppers–Lortz instability (around $\theta = 50°$ can be separated, in contrast with the case of smaller Prandtl numbers (e.g. $P_r = 5$) where all the angles $0 < \theta \leqslant 64°$ are unstable. For this rotation rate, only the small angle instability survives at Prandtl number $P_r = 15$. It becomes hardly visible at $P_r = 50$. Indeed, as the Prandtl number goes to infinity, the negative eigenvalue $\sigma^-$ has a limit, while the outer expansion $\sigma^+_{outer}$ extends towards $\theta = 0$ where it asymptotically reaches the value $\sigma^-(0)$, the inner range reducing to the vertical axis.

Figure 3 shows the variation of the instability growth rate with the rotation rate $\tau$, for $P_r = 15$ and $\epsilon = 0.1$. For $\tau = 10$, only the small angle instability is present. The Küppers–Lortz instability (again localized around $\theta = 58°$) arises for $\tau \approx 40$ and is strongly amplified as $\tau$ is increased.

Figure 4(a) displays for $\epsilon = 0.1$, the critical value of the rotation rate $\tau$ for the onset of the Küppers–Lortz instability, as a function of the Prandtl number, as long as the latter is large enough for the two instabilities to be separated. Figure 4(b) shows the most unstable angle (in degrees) for the Küppers–Lortz instability, versus the Prandtl number, for a rotation rate corresponding to the onset of the instability.

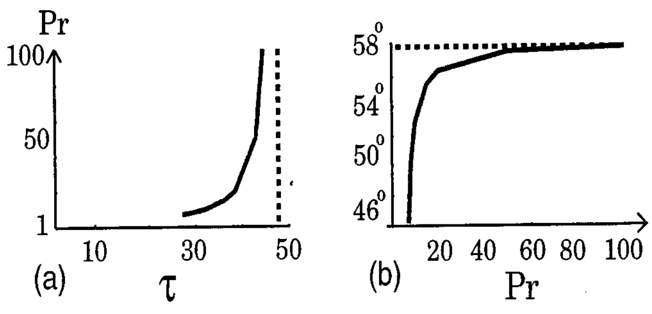


FIG. 4. Küppers–Lortz instability boundary in the $(P_r, \tau)$-plane (a), and angle associated to the unstable perturbation at the critical Taylor number versus the Prandtl number (b).

## V. NATURE OF THE INSTABILITY AND NONLINEAR DEVELOPMENTS

We showed in Section IV that in a rotating horizontal fluid layer with moderate Prandtl number, limited by top and bottom free-slip boundaries, convective rolls are linearly unstable with respect to perturbations in the form of rolls making a small angle with that of the basic pattern. This instability occurs even when the rotation rate is too low for the existence of the Küppers–Lortz instability. It is related to the divergence of the growth rate (52) which, at finite Prandtl number, occurs when the direction of the wave vector of the perturbation, approaches that of the basic rolls. We here chose the associated wave numbers to be critical, but the effect survives whatever their values.

The above instability was obtained in an infinite domain. Its persistence with lateral boundaries requires the presence of a large number of rolls, and thus a convective cell with a large aspect ratio $\mu^{-1}$. The mesh size in Fourier space scaling like $\mu$, the minimum angle $\theta$ between two wave vectors, behaves like $\mu^{1/2}$. Since for the small-angle instability $\sigma \sim \epsilon^{4/3}$ and $\theta \sim \epsilon^{2/3}$, it follows that $\sigma \sim \mu$, a growth rate intermediate between that (of order unity) of a pure amplitude instability and a phase instability, which $\sigma$ scales like $\mu^2$.

As shown in Refs. 18 and 19, in the absence of rotation, parallel rolls may also be unstable (for wave numbers larger than critical) to a skewed-varicose instability whose growth rate also varies like the inverse aspect ratio $\mu$, a scaling resulting from the strong magnitude of the mean flow in the case of free-slip boundary conditions. This instability is however not captured by the present formalism since the roll distortions involved in this instability cannot be represented within the class of perturbations (superposition of two families of straight rolls) we have considered.

In order to investigate the relation between the small-angle and the skewed-varicose instabilities, and to analyze their non-linear developments, a system of equations in the spirit of the Swift–Hohenberg equation, but coupling the leading vertical mode to the mean flow, was derived by a perturbation expansion near threshold.[15] This system which preserves the rotational invariance of the problem, generalizes equations obtained by Manneville[16] at finite Prandtl number in the absence of rotation. In a simplified version where the non-local couplings are suppressed and only a few representative nonlinear terms are retained, it is also consistent with models used in Refs. 17 and 18 for rotating convection at infinite Prandtl number. A similar model was considered in Ref. 19.

As discussed in Ref. 15, the phase equation derived in the context of the generalized Swift–Hohenberg equations, shows that the skewed varicose instability occurring without rotation near onset, becomes asymmetric with respect to the angle of the phase perturbation, in the presence of rotation. This model also shows that both the asymmetric skewed varicose and the small angle instabilities lead, by means of reconnection, to a progressive rotation of the convective rolls in the direction of the external rotation, an effect due to the mean flow which develops shear layers.

We are thus led to conclude that the small-angle divergence of the Küppers–Lortz instability growth rate pointed out in Ref. 9, results from the presence of a small-angle instability which can be identified as an asymmetric skewed-varicose instability. In contrast with the (symmetric) skewed varicose instability arising without rotation, the azymetric one developing in the presence of rotation exists whatever the value of the basic roll wave number. Both instabilities are produced by the mean flow and disappear in the limit of infinite Prandtl numbers.

## ACKNOWLEDGMENTS

We are grateful to F. Busse for suggesting the relation with the skewed varicose instability and to the anonymous referee for pointing out Ref. 19.

[1]G. Küppers and D. Lortz, ''Transition from laminar convection to thermal turbulence in a rotating fluid layer,'' J. Fluid Mech. **35**, 609 (1969).
[2]R.M. Clever and F.H. Busse, ''Nonlinear properties of convection rolls in a horizontal layer rotating about a vertical axis,'' J. Fluid Mech. **94**, 609 (1979).
[3]M.C. Cross and P.C. Hohenberg, ''Spatio-temporal chaos,'' Science **263**, 1569 (1994).
[4]L. Ning and R.E. Ecke, ''Küppers–Lortz transition at high dimensionless rotation rates in rotating Rayleigh-Bénard convection,'' Phys. Rev. E **47**, R2291 (1993).
[5]M.C. Cross, D. Meiron, and Y. Tu, ''Chaotic domains: A numerical investigation,'' Chaos **4**, 607 (1994).
[6]Y. Hu, R.E. Ecke, and G. Ahlers, ''Time and length scales in rotating Rayleigh–Bénard convection,'' Phys. Rev. Lett. **74**, 5040 (1995).
[7]F.H. Busse and K.E. Heikes, ''Convection in a rotating layer: A simple case of turbulence,'' Science **208**, 173 (1980).
[8]G. Küppers, ''The stability of steady finite amplitude convection in a rotating fluid layer,'' Phys. Lett. A **32**, 7 (1970).
[9]T. Clune and E. Knobloch, ''Pattern selection in rotating convection with experimental boundary conditions,'' Phys. Rev. E **47**, 2536 (1993).
[10]S. Chandrasekhar, *Hydrodynamic and Hydromagnetic Stability* (Oxford University Press, London, 1961).
[11]M.J. Ablowitz and D.J. Benney, ''The evolution of multi-phase modes for nonlinear dispersive waves,'' Stud. Appl. Math. **49**, 225 (1970).
[12]A.C. Newell, ''Solitons in Mathematics and Physics,'' *CBMS-NSF Regional conference series in Applied Mathematics* (SIAM, Philadelphia, 1985), Vol. 48.
[13]A. Zippelius and E.D. Siggia, ''Stability of finite-amplitude convection,'' Phys. Fluids **26**, 2905 (1983).
[14]F. H. Busse and E. W. Bolton ''Instabilities of convection rolls with stress-free boundaries near threshold,'' J. Fluid Mech. **146**, 115 (1984).
[15]Y. Ponty, T. Passot, and P.L. Sulem, ''Pattern dynamics in rotating convection at finite Prandtl number,'' in preparation.
[16]P. Manneville, ''A two-dimensional model for three-dimensional convective patterns in wide containers,'' J. Phys. **44**, 759 (1983).
[17]M. Neufeld, R. Friedrich, and H. Haken, ''Order parameter equation for high Prandtl number Rayleigh–Bénard convection in a rotating large aspect ration system,'' Z. Phys. B **92**, 243 (1993).
[18]M. Fantz, R. Friedrich, M. Bestehorn, and H. Haken, ''Pattern formation in Bénard convection,'' Physica D **61**, 147 (1992).
[19]H. Xi, J. D. Gunton, and G. A. Markish, ''Pattern formation in a rotating fluid: Küppers-Lortz instability,'' Physica A **204**, 741 (1994).